Fast Semi-automatic Target Initialization based on Visual Saliency for Airborne Thermal Imagery

Çağlar Aytekin[1], Emre Tunalı[2] and Sinan Öz[2]
[1]*Middle East Technical University, Department of Electrical and Electronics Engineering, Ankara, Turkey*
[2]*Image Processing Department, ASELSAN Inc. Microelectronics, Guidance and Electro-Optics Division, Ankara, Turkey*

Keywords: Real-time Target Initialization, Saliency, Distinctive Feature Selection, Long-term Tracking, Center-surround Histogram Difference, Error Compensation.

Abstract: In this study, a semi-automatic target initialization algorithm is introduced based on a recently proposed visual saliency approach. First, a center-surround difference based initial window selection is utilized around the input point coordinate provided by the user, in order to select the window which is most likely to contain the actual target and background satisfying piecewise connectivity. Then, a recently proposed visual saliency algorithm is exploited in order to detect the bounding box encapsulating the most salient part of the object. The experiments support that the saliency based tracking window initialization is capable of handling marking errors, i.e. erroneous user inputs, and boosts the performance of several tracking algorithms in terms of the number of frames in which successful tracking is achieved, when compared with several fixed window size initializations.

1 INTRODUCTION

Target tracking is a classical problem and has many important applications such as surveillance, activity or behavior detection. Hence, a diverse set of tracking algorithms are proposed in the literature. Majority of tracking algorithms assume predetermined target location and size for initialization of tracking (Shi and Tomasi, 1994; Sand and Teller, 2006; Ramanan et al., 2007; Dowson and Bowden, 2005; Kwon and Lee, 2010; Bibby and Reid, 2008; Grabner et al., 2010; Collins et al., 2005a; Avidan, 2007; Grabner and Bischof, 2006; Babenko et al., 2009; Grabner et al., 2008; Stalder et al., 2009). In many applications, target size and location are required as input from human-users. Therefore, target initialization can drastically change the performance of the tracker since this initial window determines for the tracker what to track, i.e. the features (Shi and Tomasi, 1994; Sand and Teller, 2006), appearance (Ramanan et al., 2007; Dowson and Bowden, 2005; Kwon and Lee, 2010), contours (Bibby and Reid, 2008). Hence, any insignificant or false information, i.e. parts of objects similar to common background or patches from background, may result in a mislearning of target appearance. Some tracking algorithms (Grabner et al., 2010; Collins et al., 2005a; Avidan, 2007; Grabner and Bischof, 2006; Babenko et al., 2009; Grabner et al., 2008; Stalder et al., 2009) try to deal with this problem inherently: They classify the foreground and background of the selected window by defining the regions close to selected window as foreground samples, and the ones distant from the selected window as background priors. Still, this attempt does not completely compensate the false initialization, specifically in scenarios with high clutter or in crowded scenes. Hence, false target initialization is still a problem. Indeed, in most of the real-time applications, erroneous input is usually provided by the user due to obligation to mark the target instantly. This erroneous input usually results in track losses prematurely. Therefore, if long-term tracking performance desired to be achieved this erroneous input should be compensated. Moreover, even in the case that user provides a perfect bounding box or the center of the target to be tracked, depending on the appearance of the target; this initialization may not always be preferred. For example, in Fig. 1(a) an object with a similar appearance with the background is illustrated. An initialization like that of in Fig. 1(b) may result in redundant features or deceptive appearance depending on the type of tracker, which may not provide long-term tracking. Therefore, we propose that target should be selected as the most salient part of an

Aytekin Ç., Tunalı E. and Öz S..
Fast Semi-automatic Target Initialization based on Visual Saliency for Airborne Thermal Imagery.
DOI: 10.5220/0004668904900497
In *Proceedings of the 9th International Conference on Computer Vision Theory and Applications* (VISAPP-2014), pages 490-497
ISBN: 978-989-758-009-3

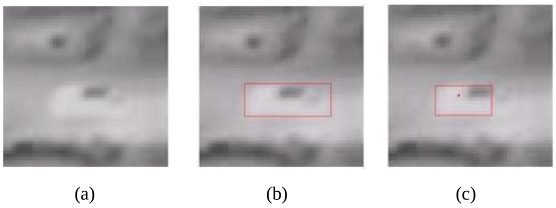

Figure 1: (a) A thermal image containing a car as a target, (b) The actual bounding box including the whole target is indicated as red, (c) The bounding box detected by the proposed target initialization algorithm.

object, most distinctive segment from background, as in Fig. 1(c), in order to achieve long-term tracking performance.

In many industrial applications the initialization of target needs to be done in real time and most of the time the only user interaction is just a marking operation on the object. Using only marking input, many systems initialize target, being target center at the marked point with predefined discrete bounding box sizes. In this study, a real-time target initialization framework is proposed which takes a single (x,y) image coordinate from the user and returns the most salient region bounding box in the neighborhood. It is also shown that this initialization results in better discriminative targets with respect to background and provides a long-term tracking even in trackers that claim to deal with discrimination problem during tracking.

Automatic target initialization methods exist in the literature, with several limitations. One main approach is motion detection (Veeraraghavan et al., 2006) which cannot deal with stationary targets. A more systematic approach is used in (Toyama and Wu, 2000), however it requires a target model. There are other existing methods (Mahadevan and Vasconcelos, 2011; Yilmaz et al., 2003) that can handle previously mentioned issues. These algorithms process exhaustive search over the entire image to extract targets which takes a lot of time, thereby making them inappropriate for real-time applications. Hence, we do not prefer exploiting these works and we follow a semi-automatic approach instead, since we are concentrated on real-time applications. Furthermore, we avoided using object window detector as (Alexe et al., 2010) or segmentation algorithms with user interaction (Rother et al., 2004), since we have obligation to select the initial bounding box in real-time and we only retain a coordinate input.

The rest of the paper is organized as follows: The proposed target initialization method is explained in Section 2, the conducted experiments are analyzed in Section 3, finally the study is concluded in Section 4 where discussions were made.

2 PROPOSED METHOD

The target initialization method proposed in this study consists of three main steps: First, an initial window selection method based on center-surround histogram difference is processed, then saliency map in this window is calculated by the method (Wei et al., 2012) and the saliency map is thresholded. Finally, the connected component having maximum total saliency with minimum distance to the center is selected as initial target location. These steps are extensively analyzed in this chapter.

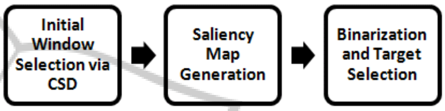
Initial Window Selection via CSD
Saliency Map Generation
Binarization and Target Selection

Figure 2: Three main steps of the proposed initial target window selection algorithm.

2.1 Initial Window Selection

The motivation of selecting an initial window is to include the foreground and to provide a feasible background for the saliency evaluation method (Wei et al., 2012) which assumes that most of the image boundaries belong to the background and the background patches are piecewise connected. This makes the saliency detection sensitive to the image boundaries; hence a proper window selection is required. The main approach to an initial window selection is based on the well-known center-surround histogram difference (CSD). First, we calculate the center-surround histogram distances in windows of multiple sizes around the pixel marked by the user. In order to ensure the piecewise connectivity assumption in the saliency detection, we choose the window which gives the first local maximum of histogram distance HD vector which is defined as follows:

$$HD(i) = K\left(B_{w_i} + F_{w_i}\right), \tag{1}$$

where K is a distance measure between B_{w_i} and F_{w_i} which are the foreground and background histograms of window w_i and $i = (1,2,.,N)$.

Local maxima other than the first one can have a larger CSD. Actually, these maxima appear in windows with layered background patches, where the background region may correspond to only some patches of real background, whereas the foreground window may cover the actual foreground together with another layer of background (See Fig. 3). However, we wish to obtain an initial window where background patches are piecewise connected, which may not be case in some local maxima other than the first

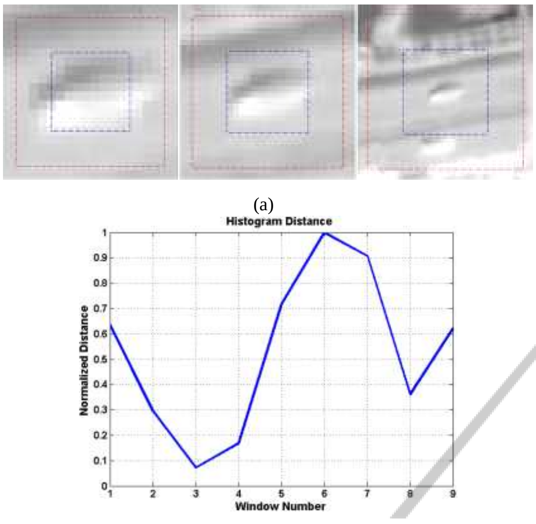

(a)

(b)

Figure 3: (a) Three window sizes and blue and red windows indicating the foreground and background region borders respectively, (b) Histogram distance of foreground and background regions obtained at each window number.

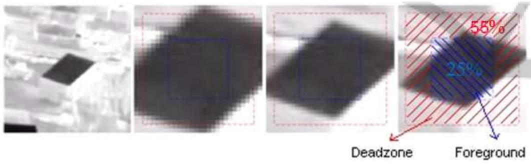

Figure 4: Foreground (blue),deadzone (red) and background borders for several window selections.

one. Therefore, we select the window corresponding to first local maximum of $HD(i)$.

During the selection of initial window, various object shapes are desired to be handled also. However, since the foreground and background regions of each window are selected as square boxes, objects with shapes deviating from a square can be problematic. For example, if foreground window is selected as encapsulating the whole target in Fig. 4, this square window also includes regions from background which decrease CSD. To compensate this effect we introduce a dead-zone region when calculating CSD. Empirically we choose the foreground and background to cover the 25 and 20 percent of the selected window area respectively and the remaining area to be a dead-zone. This selection is realized to help dealing with targets with large deviation from square shape (Fig. 4).

Another issue is the calculation of histogram distances of foreground and background. For this purpose, quadratic-chi histogram distance (Pele and Werman, 2010) is utilized, since it suits to the problem in two aspects. First, it is capable of handling quantization effects that occurs when close intensity values are mapped into different histogram bins by using similarity matrix which is taking care of cross-bin relationship. Second, it suppresses the distances resulting from bins with high values. Formulation of quadratic-chi histogram distance is given in Eqn. 2 as:

$$QC_m^A(P,Q) = \sqrt{\sum_{ij} \frac{(P_i - Q_i)}{\left(\sum_c (P_c + Q_c) A_{ci}\right)^m} \frac{(P_j - Q_j)}{\left(\sum_c (P_c + Q_c) A_{cj}\right)^m} A_{ij}}, \qquad (2)$$

where P and Q represent N dimensional nonnegative bounded foreground and background histograms, ”i,j” are histogram bins, A is the nonnegative symmetric bin similarity matrix which is NxN and m is the normalization factor retaining distance due to high bin values.

2.2 Saliency Map Calculation

The saliency map of the window, selected by the algorithm above, is extracted by a recently proposed fast saliency extraction method (Wei et al., 2012) in which the saliency problem is tackled from different perspective by focusing on background more than the object. Although there are various saliency detection algorithms (Hou and Zhang, 2007; Achanta et al., 2009; Goferman et al., 2010; Cheng et al., 2011), the main motivation of using this method is its capability of extracting a saliency map within few milliseconds; however, it has two basic assumptions that should be guaranteed, namely boundary and connectivity. The boundary assumption is reflection of a basic tendency that photographer/cameraman do not crop salient objects among the frame. Therefore, the image boundary is usually background. The connectivity assumption comes from the fact that background regions are generally tend to be large and homogenous, i.e. sky, grass. In other words, most image patches can be easily connected to each other piecewisely. Satisfying these two conditions, the salient regions are assumed to be the patches that are extracted by downscaling or by any super pixel extraction algorithm with high geodesic distance from the boundaries of the image that is assumed to correspond to piecewise-connected background regions. The geodesic saliency of a patch p is the accumulated edge weights along the shortest path from p to virtual background node b in an undirected weighted graph $p \in \{\upsilon, \varepsilon\}$,

$$S(p) = min_{p_1 = p, p_2, \ldots, p_n = b} \sum_{i=1}^{n-1} weight\,(p_i, p_{i+1}), \qquad (3)$$

$$s.t.\,(p_i, p_{i+1}) \in \varepsilon,$$

For this purpose a shortest path algorithm is exploited (Toivanen, 1996) in order to calculate the shortest distance to the image boundaries from each patch. The higher this value is the more salient the patch. Furthermore, since patches close to the center of the image requires a longer path in order to reach the background, accumulation of weights tend to be larger in the center patches. Therefore, this method also favors the center image regions as more salient which is reasonable since salient regions tend to occur around the center of image.

2.3 Binarization of Saliency Map

Since we look for a fast target initialization, we wish to keep the computational cost at minimum even in the binarization step. Hence, a fast binarization approach is proposed here exploiting the local maxima of saliency map. The threshold is selected by a weighted average of local maxima of the saliency map (Eqn. 4). In this sense, for fast binarization process, fast local maxima detection is required. In order to achieve fast local maxima detection, a fast local maxima detection algorithm (Pham, 2010) is used. After detection of local maxima, we form a vector $LocalMax_{sorted}$ by sorting the local maxima in descending order, and the normalized laplacian of this vector is used as weights for local maxima. This is meaningful since the local maxima with higher laplacian represent a distinctive fall within local maxima. We shall favor these values when calculating the threshold level since distinctive falls are indicators of split between regions with higher saliency with respect to their surroundings. Hence, a threshold would be suitable for binarization around the most distinctive fall; greatest weight is given to that local maximum in the weighted average of local maxima.

$$Thr = LocalMax_{sorted}^{T} . \nabla^2_{norm}\left(LocalMax_{sorted}\right), \quad (4)$$

where

$$\nabla^2_{norm}(f) = \frac{\nabla^2(f) - min\left(\nabla^2(f)\right)}{\sum_i \nabla^2(f)|_i - min\left(\nabla^2(f)\right)}, \quad (5)$$

In order to sort the local maxima in a fast manner, we generate a binary tree with heap property in the phase of local maxima selection. Then, sorting is accomplished in classical sense by selecting the first element,highest, and then re-ordering the heap at each turn until all local maxima are sorted.

After thresholding the saliency map, the connected component maximizing the regularization energy given by Eqn. 6, i.e. the most salient region with minimum distance to the center, is selected as the target.

$$argmax_{c_i} \frac{c_i^T s}{sqrt\left(\left(x_i - x_c\right)^2 + \left(y_i - y_c\right)^2\right)}, \quad (6)$$

where C_i is the vectorized form obtained by raster scanning the 2D label matrix with values 1 and 0 as foreground and background respectively, S is the saliency map vectorized similarly and (x_i, y_i), (x_c, y_c) are the centers of each connected component and the inital window respectively.

Based on the explainations above, the entire initial target window selection algorithm is summarized in Algorithm 1.

Algorithm 1: Semi-Supervised Target Initialization.

```
Input: $(x,y)$ coordinates from user indicating the target location roughly

Initial window selection: Given input $(x,y)$, select a square window which is most likely to include actual target and the background satisfying piecewise connectivity from a set of windows $W \in \{w_1,,w_n\}$;
Initialize $Dist = \{\}$;
for $W \in \{w_1,,w_n\}$ do
    Obtain histogram of square foreground window $F_W$: 25% of area($W$), centered at $(x,y)$
    Obtain histogram of background window $B_W$: 20% of area($W$), from the boundaries of $W$
    Calculate quadratic-chi histogram distance $HD(W) = QC_m^A(F_W, B_W)$
    $Dist = Dist \cup HD(w)$;
end for
return window size that corresponds to 1st local
    maximum of $Dist$ as initial window size
Saliency Map Calculation: Given the initial window size
return saliency map using Eqn. 3
Binarization of Saliency Map: Given the saliency map
Find local maxima and sort in descending order to obtain $LocalMax_{sorted}$
Calculate normalized laplacian of $LocalMax_{sorted}$ using Eqn. 5
Obtain the threshold Thr using Eqn. 4
Select the connected component satisfying Eqn. 6

Output: Target bounding box enclosing the selected connecting component.
```

3 EXPERIMENTS

The proposed method was tested for two aspects with two different procedures. For both stages, in initial window selection phase, nine window sizes from $20x20$ to $100x100$ with regular grid were used and histogram bin number was selected as 25. In the calculation of histogram difference, the parameters m and bin similarity matrix A were selected empirically as m

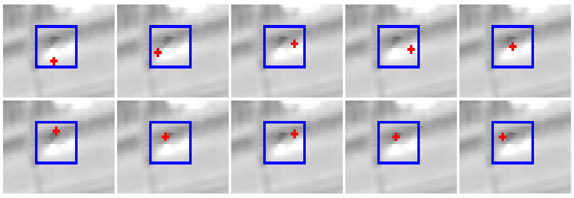

Figure 5: Erroneous marking input (red dot) and the output target window (blue bounding box).

is to be 0.5 and A to be in 5 bin neighborhood which cover one fifth of total number of bins. It should be noted that increase in the number of bins of histogram results in better resolution; therefore, better discriminability between foreground and background. However, it also yields increase in computational complexity which reduces time efficiency. Considering the compromise between time efficiency and resolution, histogram bin number was decided to be 25. The same consideration is also valid for the saliency map calculation in which 2x2 patches were used for mean intensity computation. Thus, these parameters may be modified according to system in use.

At the first experiment, proposed target initialization method and its error compensation capability, i.e. robustness to marking errors, were tested. Ground truth for performance evaluation was generated by 10 different users. 5 specific images[1] illustrated in Appendix were given to all users. They were kindly requested to generate bounding box for anything in the image that appears to them as target. After the bounding box generation, we selected targets among the images generated by at least 6 different users as targets and the ground truth of target bounding boxes were decided to be the average of all bounding boxes generated by users. Input marks were given as the summation of the center coordinates of ground truth bounding box and uniformly distributed pseudo random integers, representing marking errors, for each direction as illustrated in Fig 5.

The noise amount was decided to be 5 pixels at maximum for the targets that are smaller than 20 pixels, however for the targets which are greater than 20 pixels noise amount becomes one fourth of the target size. For each selected target, the target initialization algorithm was run for 10 times with erroneous input and numbers of successful initializations were noted. The success measure for initialization is the ratio of intersection and union of the ground truth and the target bounding box (overlap measure) and successful initialization assumed to be achieved when the measure is higher than 0.5 as it is used in many different applications. Since, the purpose is to obtain exactly same target bounding box for erroneous user input, we counted the maximum number of target bounding boxes which are exactly matched among the target bounding boxes that are considered as successfully initialized and their ratio is used for robustness measure. It should be noted that in most of cases ($\approx 87\%$) the input error was compensated by the proposed algorithm and robust target initialization(exactly same target bounding box) was achieved. Results of the first part are given in Table 1.

Table 1: Performance of proposed method for target initialization and marking error compansation.

Image& Target No		# of Succesful Target Initilization (for 10 trial)	Max # of Fully Matched Target Window
1	1	10	10
	2	10	10
	3	10	10
	4	9	9
	5	10	10
	6	10	10
	7	0	X
	8	9	2
	9	10	10
	10	10	10
	11	6	5
	12	9	2
	13	0	X
2	1	10	10
	2	9	9
	3	10	10
	4	9	5
	5	7	6
	6	0	X
	7	10	10
	8	10	10
3	1	0	X
	2	0	X
	3	9	7
	4	10	10
	5	0	X
4	1	10	10
	2	10	8
	3	10	10
	4	10	10
	5	10	10
	6	10	10
	7	10	10
	8	10	10
	9	9	3
	10	10	10
	11	0	X
	12	10	10
	13	10	10
	14	0	X
5	1	10	8
	2	7	7
	3	10	6
	4	5	5
	5	0	X
	6	10	7
	7	3	3
	8	10	6
	9	10	6
Initialization Performance:			**75.7**
Robustness:			**87.3**

At the second stage of experiments we tested the effect of our target initialization algorithm on tracking by evaluating the tracking performance of three tracking algorithms (Grabner and Bischof, 2006; Grabner et al., 2008; Stalder et al., 2009) in terms of the number of frames that the tracker successfully tracks against the condition that the distance from the center of the object to be tracked to the target window center

[1] To obtain detailed results and the input images, please contact with the authors.

does not change more than 5 pixels. The marking input was given with a random error similar to previous stage but in this case initialization and tracking was executed only once. We compared the performance of the proposed algorithm with that of fixed window size initializations, which is the case for many real-time applications. 16*x*16, 32*x*32 and 64*x*64 window sizes were used whose centers marked by the user. It should be mentioned that initializing the target 5 pixels wider than extracted window by the proposed algorithm at each direction helps the trackers to learn the model of foreground better, hence we chose the initial windows wider. The experiments were conducted over various datasets from the work of Collins et al. (Collins et al., 2005b) with several scenarios which includes airborne videos. Before comparing the tracking performances, we first analyzed the location of the initialization window determined by the proposed algorithm when initial marks provided by the user were erroneous, i.e. far from the center of the target. In Fig. 6 the marks and the proposed target windows are illustrated. As it is realized, the algorithm is quite tolerant to erroneous input and achieves high performance of selecting the salient part of the target. On the other hand, when the tracking window was selected with fixed size target initialization, the initial window tended to include various parts of background image, decreasing the tracking performance. The tracking performance evaluations in terms of unsuccessful frame numbers are given in Table 2. In this sense, 0 means target is successfully tracked throughout the scenario.

We observed that the proposed initialization achieved high mean performance over the scenarios when compared with that of each fixed size initializations, and it gave comparable results with each single window initialization almost in each scenario. The performance boost achieved with the proposed algorithm results from handling a subset of scenarios very well such as crowded scenes, where target is surrounded with many objects; or a small part of background around the neighborhood of the target including very strong, discriminative features. In the former case, a erroneous initialization may result in tracking ”jumps” where the tracker starts to track the other target, whereas in the latter case, the tracker may learn the discriminative features as the ones that belong to background and not the actual target. Both cases occur if the window is selected large or localized at an erroneous position from wrong marking. On the other hand, a small window initialization may prevent the tracker to learn the features discriminative enough to track the target, resulting in the loss of track. The proposed initialization is able to compensate for such effects and achieves good performance. Furthermore, in cases of occlusion and illumination changes, we observed that the tracker is more likely to redetect the target and continues tracking. Although redetecting target is a trait of the tracking algorithm itself, a more discriminative initial target window selection is observed to help boosting the performance in these scenarios.

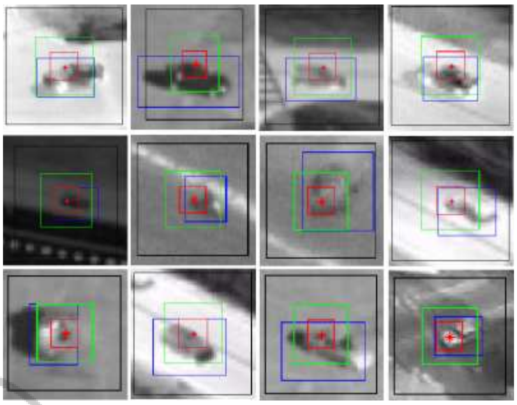

Figure 6: Some examples of target initialization windows: (black)64x64 window, (green) 32x32 window, (red) 16x16 window, (blue) window extracted by the proposed method and the red asterisk is the click input provided by the user.

The algorithm is applicable to real-time and a C++ implementation of the proposed target initialization algorithm takes about 12 ms on average in TMS320C6713 Floating-Point Digital Signal Processor @270 MHz which is enough to achieve target initialization in a frame for 60 fps systems.

4 CONCLUSIONS

In this work, we have shown that target initialization can dramatically change the performance of the tracker, since the initial window determines for the tracker what to track. In order to achieve a better tracking performance; we proposed a fast, saliency based algorithm for target initialization. Performance boost of tracker is mainly based on two key features of target initialization algorithm: It is capable of compensating erroneous user input; also selecting the most distinctive, salient part of object as target, so better discrimination is achieved between the target and background. Experimental results show that tracking performance is boosted in scenarios, in which the tracking is initialized by the proposed algorithm. Very low computational cost and requirement of only a point coordinate as input in the neighborhood of the target make this approach preferable in real time tracking applications.

Table 2: Performance comparison of proposed method and fixed sized windows for three different trackers.

Scenario			**BooostingTracker (Grabner and Bischof, 2006)**				**SemiBooostingTracker (Grabner et al., 2008)**				**BeyondSemiBooostingTracker (Stalder et al., 2009)**			
Sequence	**Initial Frame**	**Frames**	**Proposed**	**16x16**	**32x32**	**64x64**	**Proposed**	**16x16**	**32x32**	**64x64**	**Proposed**	**16x16**	**32x32**	**64x64**
1.pktest01	0	450	315	310	307	**210**	274	314	299	**191**	**157**	178	275	241
2.pktest01	1110	350	76	316	**0**	155	**14**	74	63	194	80	160	**78**	344
3.pktest02	0	470	**431**	434	433	438	**213**	437	376	197	202	206	231	**193**
4.pktest02	770	450	**0**	**0**	**0**	388	360	372	**275**	373	**0**	192	102	33
5.pktest02	1185	330	**32**	279	96	103	**5**	8	52	262	**84**	148	273	116
6.egtest03	0	300	**0**	300	267	16	**237**	300	300	240	**29**	300	39	72
7.pktest03	290	230	191	190	**185**	188	196	192	**103**	184	**139**	197	139	199
8.egtest01	0	150	**0**	150	150	**0**	**0**	150	150	**0**	59	150	150	**40**
9.egtest03	0	150	**0**	11	137	77	**52**	57	141	71	**47**	150	74	38
10.pktest03	0	415	86	86	**80**	122	**83**	88	118	210	94	410	**88**	186
Average number of frames with track loss			**116.11**	221.11	175.00	175.00	**150.11**	211.56	195.44	190.22	**88.56**	186.78	151.22	141.78

Although a dead zone was introduced in order to deal with elongated objects, the proposed window selection method may not be effective for all elongated objects. Specifically, when significant amount of the object pixels flood into the background zone together with background pixels in foreground zone affect target initialization adversely and may yield erroneous target initialization, which may be the case for elongated objects. Even though the experiments are executed in thermal data sets in which target objects has smooth transition due to heat diffusion equation, the suggested solution may be well generalized to other imaging devices.

REFERENCES

Achanta, R., Hemami, S., Estrada, F., and Susstrunk, S. (2009). Frequency-tuned salient region detection. In *Computer Vision and Pattern Recognition, 2009. CVPR 2009. IEEE Conference on*, pages 1597–1604.

Alexe, B., Deselaers, T., and Ferrari, V. (2010). What is an object? In *Computer Vision and Pattern Recognition (CVPR), 2010 IEEE Conference on*, pages 73–80.

Avidan, S. (2007). Ensemble tracking. *Pattern Analysis and Machine Intelligence, IEEE Transactions on*, 29(2):261–271.

Babenko, B., Yang, M.-H., and Belongie, S. (2009). Visual tracking with online multiple instance learning. In *Computer Vision and Pattern Recognition, 2009. CVPR 2009. IEEE Conference on*, pages 983–990.

Bibby, C. and Reid, I. (2008). Robust real-time visual tracking using pixel-wise posteriors. In *Proceedings of the 10th European Conference on Computer Vision: Part II*, ECCV ’08, pages 831–844, Berlin, Heidelberg. Springer-Verlag.

Cheng, M., Zhang, G., Mitra, N. J., Huang, X., and Hu, S. (2011). Global contrast based salient region detection. In *Proceedings of the 2011 IEEE Conference on Computer Vision and Pattern Recognition*, CVPR ’11, pages 409–416, Washington, DC, USA. IEEE Computer Society.

Collins, R., Liu, Y., and Leordeanu, M. (2005a). Online selection of discriminative tracking features. *Pattern Analysis and Machine Intelligence, IEEE Transactions on*, 27(10):1631–1643.

Collins, R., Zhou, X., and Teh, S. K. (2005b). An open source tracking testbed and evaluation web site. In *IEEE International Workshop on Performance Evaluation of Tracking and Surveillance (PETS 2005), January 2005*.

Dowson, N. D. H. and Bowden, R. (2005). Simultaneous modeling and tracking (smat) of feature sets. In *Computer Vision and Pattern Recognition, 2005. CVPR 2005. IEEE Computer Society Conference on*, volume 2, pages 99–105.

Goferman, S., Zelnik-Manor, L., and Tal, A. (2010). Context-aware saliency detection. In *Computer Vision and Pattern Recognition (CVPR), 2010 IEEE Conference on*, pages 2376–2383.

Grabner, H. and Bischof, H. (2006). On-line boosting and vision. In *Computer Vision and Pattern Recognition, 2006 IEEE Computer Society Conference on*, volume 1, pages 260–267.

Grabner, H., Leistner, C., and Bischof, H. (2008). Semi-supervised on-line boosting for robust tracking. In *Proceedings of the 10th European Conference on Computer Vision: Part I*, ECCV ’08, pages 234–247, Berlin, Heidelberg. Springer-Verlag.

Grabner, H., Matas, J., Van Gool, L., and Cattin, P. (2010). Tracking the invisible: Learning where the object might be. In *Computer Vision and Pattern Recognition (CVPR), 2010 IEEE Conference on*, pages 1285–1292.

Hou, X. and Zhang, L. (2007). Saliency detection: A spectral residual approach. In *Computer Vision and Pattern Recognition, 2007. CVPR ’07. IEEE Conference on*, pages 1–8.

Kwon, J. and Lee, K. M. (2010). Visual tracking decomposition. In *CVPR*, pages 1269–1276.

Mahadevan, V. and Vasconcelos, N. (2011). Automatic initialization and tracking using attentional mechanisms. In *Computer Vision and Pattern Recognition Workshops (CVPRW), 2011 IEEE Computer Society Conference on*, pages 15–20.

Pele, O. and Werman, M. (2010). The quadratic-chi histogram distance family. In *Proceedings of the 11th European conference on Computer vision: Part II*, ECCV’10, pages 749–762, Berlin, Heidelberg. Springer-Verlag.

Pham, T. Q. (2010). Non-maximum suppression using fewer than two comparisons per pixel. In Blanc-Talon, J., Bone, D., Philips, W., Popescu, D., and Scheunders, P., editors, *Advanced Concepts for Intelligent Vision Systems*, volume 6474 of *Lecture Notes in Computer Science*, pages 438–451. Springer Berlin Heidelberg.

Ramanan, D., Forsyth, D., and Zisserman, A. (2007). Tracking people by learning their appearance. *Pattern Analysis and Machine Intelligence, IEEE Transactions on*, 29(1):65–81.

Rother, C., Kolmogorov, V., and Blake, A. (2004). ”grabcut”: interactive foreground extraction using iterated graph cuts. In *ACM SIGGRAPH 2004 Papers*, SIGGRAPH ’04, pages 309–314, New York, NY, USA. ACM.

Sand, P. and Teller, S. (2006). Particle video: Long-range motion estimation using point trajectories. In *Computer Vision and Pattern Recognition, 2006 IEEE Computer Society Conference on*, volume 2, pages 2195–2202.

Shi, J. and Tomasi, C. (1994). Good features to track. In *Computer Vision and Pattern Recognition, 1994. Proceedings CVPR ’94., 1994 IEEE Computer Society Conference on*, pages 593–600.

Stalder, S., Grabner, H., and Van Gool, L. (2009). Beyond semi-supervised tracking: Tracking should be as simple as detection, but not simpler than recognition. In *Computer Vision Workshops (ICCV Workshops), 2009 IEEE 12th International Conference on*, pages 1409–1416.

Toivanen, P. J. (1996). New geodesic distance transforms for gray-scale images. *Pattern Recogn. Lett.*, 17(5):437–450.

Toyama, K. and Wu, Y. (2000). Bootstrap initialization of nonparametric texture models for tracking. In *Proceedings of the 6th European Conference on Computer Vision-Part II*, ECCV ’00, pages 119–133, London, UK, UK. Springer-Verlag.

Veeraraghavan, H., Schrater, P., and Papanikolopoulos, N. (2006). Robust target detection and tracking through integration of motion, color, and geometry. *Computer Vision and Image Understanding*, 103(2):121–138.

Wei, Y., Wen, F., Zhu, W., and Sun, J. (2012). Geodesic saliency using background priors. In *Proceedings of the 12th European conference on Computer Vision - Volume Part III*, ECCV’12, pages 29–2, Berlin, Heidelberg. Springer-Verlag.

Yilmaz, A., Shafique, K., and Shah, M. (2003). Target tracking in airborne forward looking infrared imagery. *Image and Vision Computing*, 21(7):623 – 635.

APPENDIX

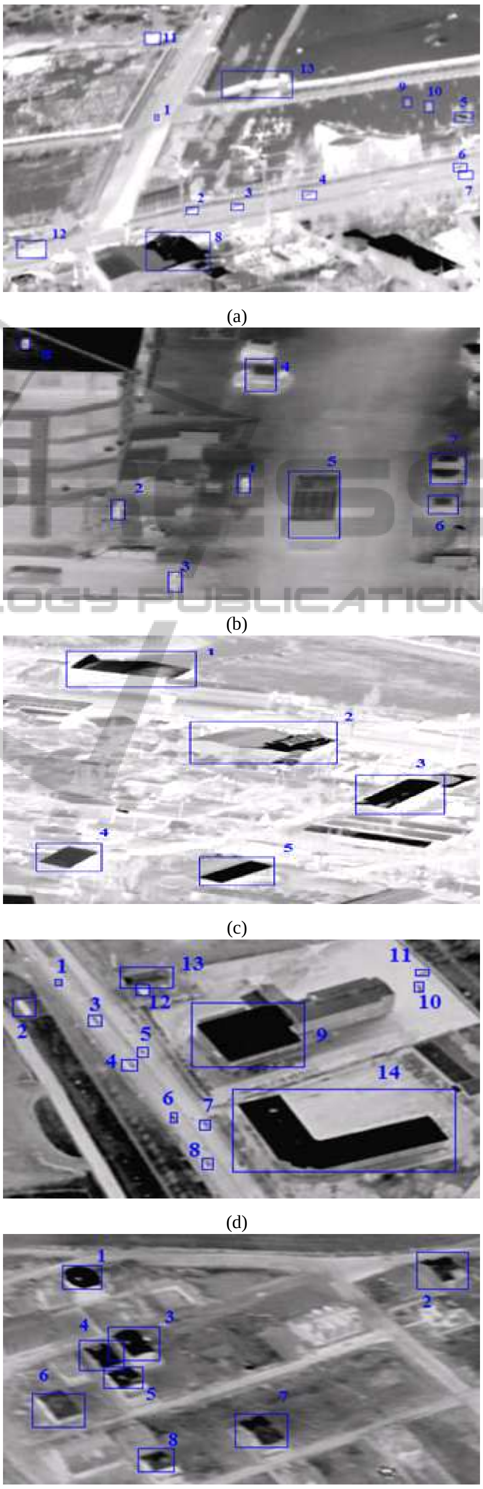

(a)

(b)

(c)

(d)

(e)

Figure 7: Thermal image dataset.